

Chemistry

MICROWAVE-ASSISTED SYNTHESIS OF LANTHANIDE HEXABORIDES:  
FORMATION OF  $\text{LaB}_6$ ,  $\text{PrB}_6$  AND CHALLENGES  
WITH HEAVIER LANTHANIDES

A. M. AGHOYAN \*

*A.B. Nalbandyan Institute of Chemical Physics, NAS of the RA, Armenia*

Rare-earth hexaborides ( $\text{RB}_6$ ) are attractive materials for photonic, electronic, and energy applications owing to their unique crystal and electronic structures. Conventional synthesis methods, however, are limited by very high temperatures, long reaction times, and the use of complex precursors. In this work, we report a rapid and energy-efficient microwave-assisted synthesis (MS) method for the preparation of  $\text{RB}_6$  powders. Using simple precursors (lanthanide oxides and elemental boron), hexaborides of La and Pr were successfully obtained within only 10 min, despite the thermodynamic constraints of the  $\text{R}_2\text{O}_3/\text{B} \rightarrow \text{RB}_6$  reaction systems. Structural and morphological characterizations (XRD, XPS, SEM/EDS) confirmed the formation of highly crystalline cubic phases with uniform particle sizes in the 1–5  $\mu\text{m}$  range. For heavier lanthanides (Gd, Ho, Er), mixed boride and borate phases were observed instead of pure hexaborides. These results demonstrate the potential of MS for overcoming thermodynamic barriers and enabling fast, energy-efficient synthesis of selected lanthanide hexaborides.

<https://doi.org/10.46991/PYSUB.2025.59.3.084>

**Keywords:** microwave-assisted synthesis, rare-earth hexaborides, lanthanide borides, refractory materials.

**Introduction.** Rare-earth hexaborides ( $\text{RB}_6$ , R = lanthanide, Sc, Y) are an important class of refractory materials distinguished by their unique crystal structures and strong covalent B–B bonding within stable boron octahedral frameworks. These materials exhibit a remarkable combination of physical and chemical properties, including low work functions ( $\text{LaB}_6 \approx 2.74$  eV,  $\text{CeB}_6 \approx 2.5$  eV,  $\text{GdB}_6 \approx 1.5$  eV), high thermal and electrical conductivities, low thermal expansion coefficients, and high melting points ( $\text{GdB}_6 - 2510^\circ\text{C}$ ) [1–6]. Such features have led to diverse applications, ranging from high-energy optical systems [1], electron emission cathodes [3, 7], and high-resolution detectors [2] to potential roles in energy technologies such as solid absorbers for concentrating solar power (CSP) systems [8].

Despite their attractive properties, which arise from the embedding of rare-earth metal atoms within a stable boron octahedral network that governs their electronic structure, the synthesis of  $\text{RB}_6$  compounds remains highly challenging. Conventional methods, including solid-state reactions (borothermal and

---

\* E-mail: [artur.aghoyan@gmail.com](mailto:artur.aghoyan@gmail.com)

carbothermal reductions) [9–13], electrolysis in molten salts [14–16], vapor-phase deposition including chemical and physical vapor deposition (CVD and PVD) [17–21], and combustion/self-propagating high-temperature synthesis (SHS) [22–24], typically require very high reaction temperatures ( $>1200^{\circ}\text{C}$ ), long processing times (often several hours), or multi-step procedures. For example, the borothermal reduction of  $\text{CeO}_2$  with boron proceeds at  $1200\text{--}1800^{\circ}\text{C}$  under vacuum [25], while carbothermal routes at  $1600^{\circ}\text{C}$  leave residual carbon impurities [26]. Even alternative “low-temperature” syntheses, such as reactions involving nitrates and boron oxide in sealed reactors [27], are time-intensive and rely on complex precursors. These drawbacks hinder the scalable production of  $\text{RB}_6$  powders with high purity and controlled particle sizes.

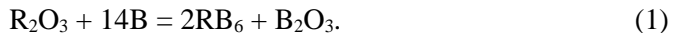
The challenge is even more pronounced for heavy or late lanthanide hexaborides (e.g.,  $\text{PrB}_6$ ,  $\text{GdB}_6$ ,  $\text{HoB}_6$ ,  $\text{ErB}_6$ ), which are more difficult to obtain due to the stronger stability of their oxides and the higher energy requirements for boride formation. As a result, reliable and efficient synthesis routes for these systems remain scarce in the literature.

Microwave-assisted synthesis (MS) offers a promising alternative. Microwave heating has emerged as an efficient and sustainable method for the preparation of advanced ceramics, carbides, and borides. Unlike conventional heating, MS enables volumetric and selective energy transfer, which dramatically accelerates solid-state reaction kinetics [28], reduces processing temperatures, and yields fine, homogeneous powders in significantly shorter times. Although microwave-assisted methods have been successfully applied to transition metal borides and carbides [29, 30], their application to rare-earth hexaborides has not yet been reported.

In this work, we investigate for the first time the feasibility of synthesizing a series of rare-earth hexaborides, with a particular emphasis on heavy lanthanide members such as  $\text{PrB}_6$ ,  $\text{GdB}_6$ ,  $\text{HoB}_6$ , and  $\text{ErB}_6$ , using a microwave-assisted solid-state route. By employing simple and readily available precursors (lanthanide oxides and elemental boron), we aim to establish a rapid, energy-efficient, and scalable synthesis method capable of overcoming the limitations of traditional approaches.

### Experimental Part.

**Materials and Methods.** The synthesis of hexaborides was done by taking the stoichiometric ratio of raw materials by general Eq. (1):



As precursors powders of high purity  $\text{R}_2\text{O}_3$  oxides (of  $\text{Pr}_2\text{O}_3$ ;  $\text{Gd}_2\text{O}_3$ ;  $\text{Ho}_2\text{O}_3$  and  $\text{Er}_2\text{O}_3$ ), (Carl ROTH GmbH+Co.KG–99.5%, p.a.) and B (99.5%, particle size about  $0.5\text{ }\mu\text{m}$ ) were used. The powders containing stoichiometrically calculated  $\text{R}_2\text{O}_3$  and B (w/w) were weighed and placed in a glass flask and mixed with a magnetic stirrer for 20 min, then homogenized by hand in an agate mortar for 5 min. The detailed mass ratios of raw materials are listed in Tab. 1. Afterward, the initial mixture was completely transferred into a quartz (silica glass) flow reactor and was purged with high purity (99.99%, 25 mL/min) helium at room temperature for at least 30 min to ensure an inert atmosphere. Then the reaction mixture was placed in the bottom of the quartz reactor and the tube was vertically inserted into the microwave oven (MW oven: Electrolux, Type E 3, 2.45 GHz, 900 W) through an opening, a detailed quartz flow reactor-MW oven setup sketch is described in our earlier

works [31]. The mixture was subjected to microwave irradiation at 900 W up to incandescence and the irradiation was kept for over 10 min until the end of the reaction. The average temperature of the incandescence area was measured to be about 900–1050°C by an optical pyrometer (Dostman HT-1800) through a special hole made in the rear wall of the MW oven. Continuously flowing helium (25 mL/min) was used during the synthesis.

Table 1

*Stoichiometric weight proportions of raw materials calculated on the synthesis of 5 g final product*

N	Raw materials	w/w, g/g
1	$\text{Pr}_2\text{O}_3/\text{B}$	3.98/1.86
2	$\text{Gd}_2\text{O}_3/\text{B}$	4.06/1.72
3	$\text{Ho}_2\text{O}_3/\text{B}$	4.1/1.67
4	$\text{Er}_2\text{O}_3/\text{B}$	4.1/1.65

The final products after synthesis were treated with 5% NaOH solution and then washed with deionized water several times to ensure the complete removal of by-product boron oxide ( $\text{B}_2\text{O}_3$ ). The residual boron oxide and  $\text{Na}^+$  ions were analyzed (controlled) in the last portion of water by ICPMS. The residues were filtered and dried in an oven at  $105 \pm 0.5^\circ\text{C}$  for 4 h.

The crystallinity and phase composition of the materials were determined by X-ray diffraction (XRD, Rigaku, MiniFlex 600). Step-scan data were collected with  $\text{CuK}\alpha$  ( $\lambda = 1.5406 \text{ \AA}$ ) radiation, operated at 40 kV – 15 mA. Morphologies and microstructures of the samples were analyzed with the help of scanning electron microscope (SEM, EIM QUANTA 200) equipped with energy dispersive spectrometer (EDS). XPS spectra of the surface layers were recorded on an OMICRON ESCA + spectrometer (OMICRON, Germany). The pressure in the chamber of the OMICRON ESCA + analyzer was maintained below  $8 \cdot 10^{-10} \text{ mbar}$ , the radiation source was an Al anode ( $\text{AlK}\alpha$  1486.6 eV).

**Results and Discussion.** According to the results of the characterization of the synthesized  $\text{RB}_6$  powders, it was shown that the series of lanthanides of our interest, from the point of view of microwave-assisted synthesis, can be divided into two subgroups: lanthanides La, Pr (in this study), which mainly form hexaboride phases, and lanthanides Gd, Ho, Er, which form mixed boride and other phases.

**The Thermodynamic Calculations.** Before conducting the MS synthesis experiments, thermodynamic calculations were carried out using HSC 10 software. Currently, available data in the literature on the formation of lanthanide boride are only for the two lanthanide hexaboride systems of our interest, and obtained calculation results are shown in Tab. 2.

Table 2

*The value of the enthalpy and the change in Gibbs function for the formation of hexaborides from the corresponding oxides and boron at 1100°C*

N	Reactions at 1100°C	$\Delta G, \text{ kcal/mol}$	$\Delta H, \text{ kcal/mol}$
1	$\text{La}_2\text{O}_3 + 14\text{B} = 2\text{LaB}_6 + \text{B}_2\text{O}_3$	+77.5	+70.8
2	$\text{Gd}_2\text{O}_3 + 14\text{B} = 2\text{GdB}_6 + \text{B}_2\text{O}_3$	+46.3	+77.0

As we can see from Tab. 2, the reactions between rare-earth metal oxide and boron have positive values of changes in Gibbs function and enthalpy, which does not always “facilitate” the reaction. This may explain the need for high temperatures during conventional heating for these reactions to occur. Nevertheless, the unique interaction between microwaves and reactants [32] enables such reactions to proceed, leading to the formation of  $\text{RB}_6$  compounds.

**The Possibility of MS Synthesis of Thermodynamically Prohibited Lanthanide Hexaborides and Temporal Effect Study of Microwave Irradiation.** Considering the thermodynamic calculation results (Tab. 2), the  $\text{La}_2\text{O}_3/\text{B}$  reaction system has the highest positive values of changes in enthalpy and Gibbs energy ( $\Delta H = +70.8 \text{ kcal/mol}$ ,  $\Delta G = +77.5 \text{ kcal/mol}$ ), which means that this reaction is the most thermodynamically prohibited. Therefore, the reaction system  $\text{La}_2\text{O}_3/\text{B}$  was chosen as a reference to study the possibility of MS synthesis of lanthanide hexaborides/borides and the temporal effect of microwave irradiation. The mixture of the same amount of raw material was heated under the same conditions as described above. The mixtures of raw materials were irradiated at 0, 5, 10, 15, and 25-minute time intervals. The microwave heating period was fixed from the moment of incandescence of the sample (about  $1050^\circ\text{C}$ ). The XRD and SEM analyses were conducted to monitor the formation of hexaboride phases irradiated at different time intervals. Fig. 1 shows the comparative XRD patterns, and Fig. 2, a–d, show SEM images of the final products in the case of  $\text{LaB}_6$  synthesis formulation, irradiated at different times.

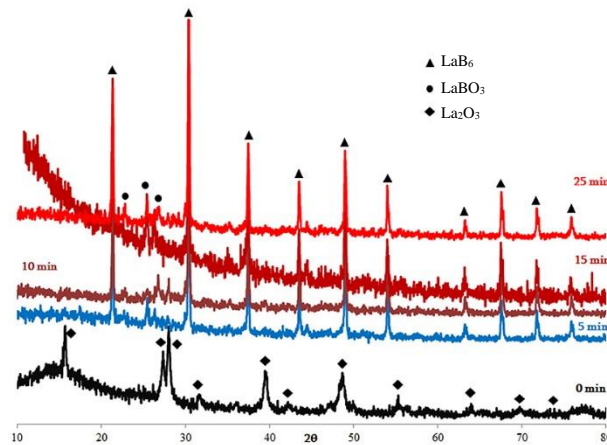


Fig. 1. Comparative XRD patterns of  $\text{LaB}_6$  samples irradiated at different time intervals: 0, 5, 10, 15, and 25 min.

The comparison of XRD patterns shows that after 5 min of irradiation a cubic  $\text{LaB}_6$  phase is formed (Powder Diffraction File, PDF# 34-0427) at the same time, very low-intensity lines of  $\text{LaBO}_3$  (PDF# 12-0762) are observed. The peak half-width and intensities of formed hexaboride do not change significantly when heated over long periods. From the SEM images it is clear that the cubic crystals are formed in the first 5 min of irradiation (Fig. 2, b), and the morphology of the samples does not change significantly over long periods of irradiation – 10 min and 25 min (Fig. 2, c and d).

Based on the temporal effect investigation, 10 min of MW irradiation was selected as the optimal synthesis time for further studies.

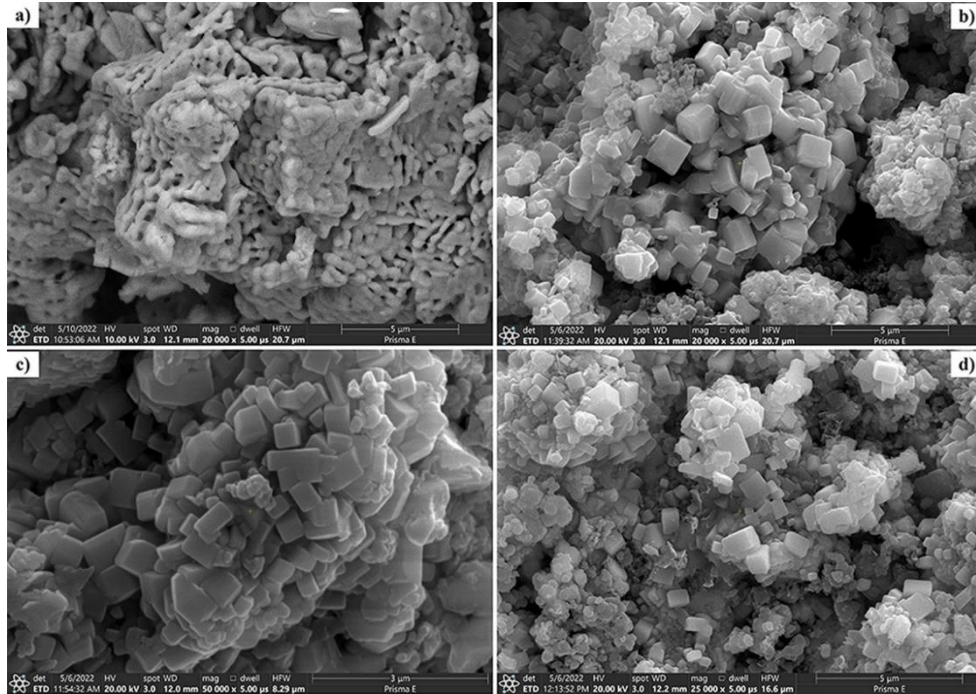


Fig. 2. SEM images of  $\text{LaB}_6$  samples irradiated at different time intervals:  
 a) 0 min (initial mixture); b) 5 min; c) 10 min; d) 25 min.

**The Characterization of MS Hexaborides.** The crystallinity and phase purity of the obtained powders were characterized by XRD. The XRD patterns were compared with the Joint committee on powder diffraction files (JCPDS) and identified with MDI/JADE software. The XRD analysis of washed powders shows that not in all  $\text{R}_2\text{O}_3/\text{B}$  reaction systems, the final phase is hexaboride, but also tetraborides, dodecaborides and other phases, although the initial mixture was prepared on hexaboride's stoichiometry.

In Fig. 3 XRD patterns of synthesized hexaboride/other boride powders are shown. The XRD results show that the final phases are mainly hexaborides for  $\text{Pr}_2\text{O}_3/\text{B}$  system and gradually hexaboride phases are decreasing starting from Gd to Er forming various boride phases. In Fig. 3-a, the XRD pattern shows intense lines of  $\text{PrB}_6$  (PDF# 38-1421), low-intensity lines of  $\text{PrBO}_3$  (PDF# 23-1384), and  $\text{Pr}(\text{BO}_2)_3$  (PDF# 23-1385). The XRD analysis of the reaction system of  $\text{Gd}_2\text{O}_3/\text{B}$  (Fig. 3-b) shows  $\text{GdB}_6$  intense lines (PDF# 65-1823, 38-1424) and comparably intense lines of  $\text{GdBO}_3$  (PDF# 13-0483). As can be seen, the amount of hexaboride phase decreased and the amount of borate ( $\text{GdBO}_3$ ) phase instead increased compared to previous  $\text{La}_2\text{O}_3/\text{B}$  and  $\text{Pr}_2\text{O}_3/\text{B}$  reaction systems (Fig. 1 and Fig. 3-a, accordingly).

The further XRD investigation of the reaction systems of  $\text{Ho}_2\text{O}_3/\text{B}$  and  $\text{Er}_2\text{O}_3/\text{B}$  shows that the main phase is not hexaboride at all (Figs. 3-c, 3-d). In Fig. 3-c, XRD pattern includes low-intensity lines corresponding to  $\text{HoB}_6$  (PDF# 25-0375), intense lines of  $\text{HoB}_4$  (PDF# 25-0377), also detected lines of  $\text{HoB}_{12}$  (PDF# 12-0103) and  $\text{HoBO}_3$  (PDF# 13-0478). The XRD pattern of the  $\text{Er}_2\text{O}_3/\text{B}$

synthesis product is presented in Fig. 3-d, and lines of  $\text{ErB}_4$  (PDF# 41-1313, 65-4928, 24-1077),  $\text{ErB}_{12}$  (PDF# 24-1076),  $\text{ErBO}_3$  (PDF# 13-0486), and non-reacted  $\text{Er}_2\text{O}_3$  (PDF# 65-3175, 65-9087) are observed.

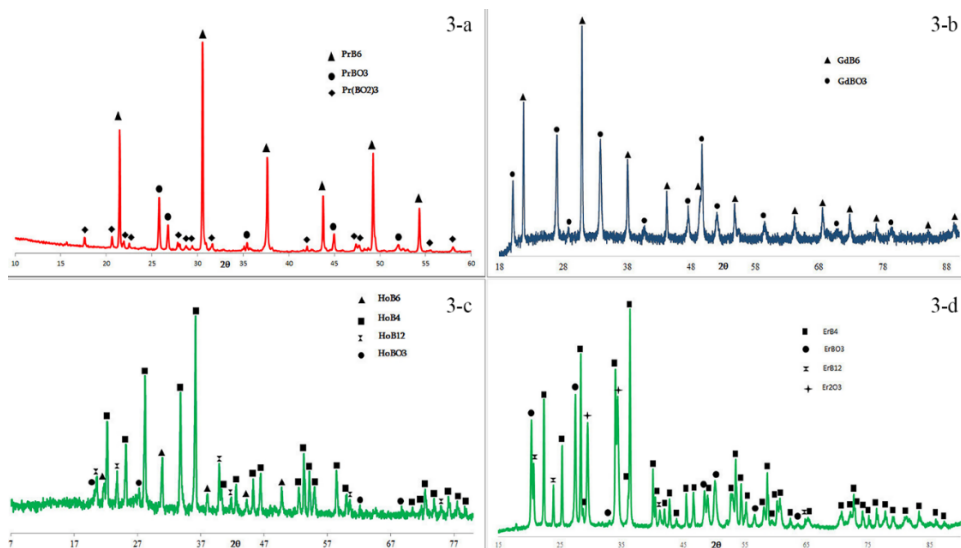


Fig. 3. XRD patterns of the obtained hexaboride and mixed boride phases:  
3-a –  $\text{PrB}_6$ ; 3-b –  $\text{GdB}_6$ ; 3-c –  $\text{HoB}_x$ , and 3-d –  $\text{ErB}_x$ .

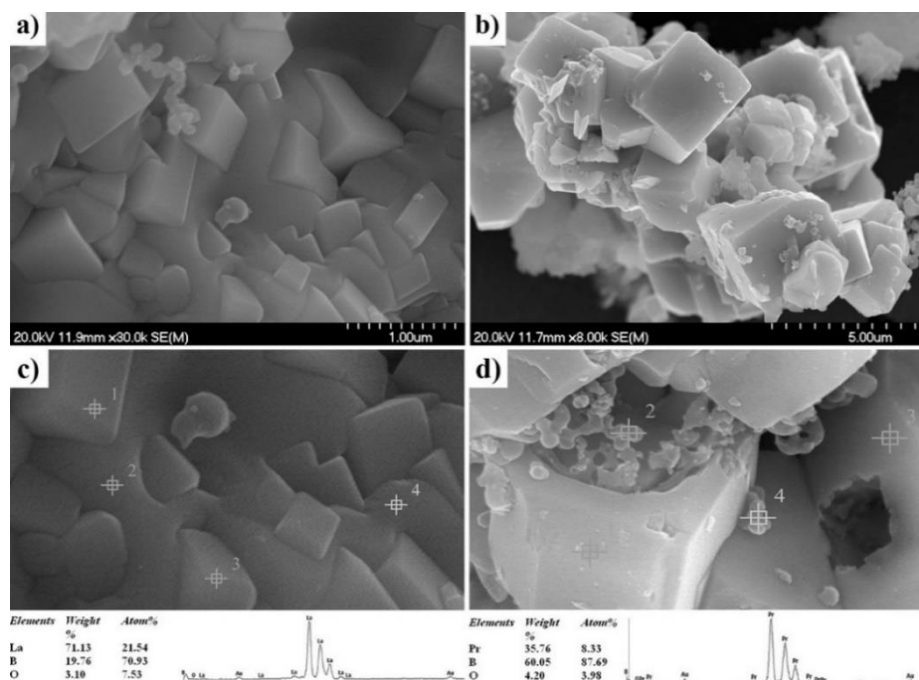


Fig. 4. SEM images of microwave-synthesized samples: a)  $\text{LaB}_6$ ; b)  $\text{PrB}_6$ ; EDS elemental mapping of c)  $\text{LaB}_6$  and d)  $\text{PrB}_6$ .

The XRD results indicate that, under identical MS conditions, only La and Pr form hexaborides as the predominant phases. Beginning with the  $\text{Gd}_2\text{O}_3/\text{B}$  reaction system, the fraction of hexaboride phases decreases progressively. For  $\text{Ho}_2\text{O}_3/\text{B}$ , the dominant product is the lower boride  $\text{HoB}_4$ , while in the  $\text{Er}_2\text{O}_3/\text{B}$  system no hexaboride phase is detected. It is noteworthy that the XRD patterns of  $\text{LaB}_6$  and  $\text{PrB}_6$  exhibit sharp and well-defined peaks (half-width  $\approx 0.2^\circ$ ), indicative of highly crystalline materials. This further suggests that the crystallite sizes of the obtained products exceed 500 Å. The morphologies and microstructures of the synthesized lanthanide hexaborides ( $\text{LaB}_6$  and  $\text{PrB}_6$ ) were investigated by SEM (Figs. 4, a and b). The images reveal the formation of well-defined cubic crystals, characteristic of  $\text{RB}_6$  structures. As shown in Fig. 4, the particle sizes of the examined hexaborides are comparable, with cubic crystals ranging from approximately 1  $\mu\text{m}$  to 5  $\mu\text{m}$ .

The EDS analysis was used to characterize the surface chemical composition of the samples. The EDS map analysis of  $\text{LaB}_6$  and  $\text{PrB}_6$  samples presented in Fig. 4, c and d, accordingly. The surface area reveals the presence of  $\text{R} = \text{La, Pr}$  as well as B and O elements in  $\text{RB}_6$  samples, where R and B are dominant. The EDS results coincide with the XRD results of the same samples, where the residues of borate phases were detected (Figs. 1 and 3-a). The presence of the borate phase suggested being a result of oxidation of the powder's surface, as it had been established earlier [33] or an incomplete reaction (as intermediate phase from solid phase reaction of  $\text{R}_2\text{O}_3/\text{B}$  system [11]).

A comparison of the XRD, SEM and EDS analysis results shows that La and Pr form hexaborides with borate phases (perceivable amounts of borate phase are seen in the case of  $\text{LaB}_6$ ). To investigate the location of borates in La and Pr hexaborides samples X-ray photoelectron spectra (XPS) analysis was done.

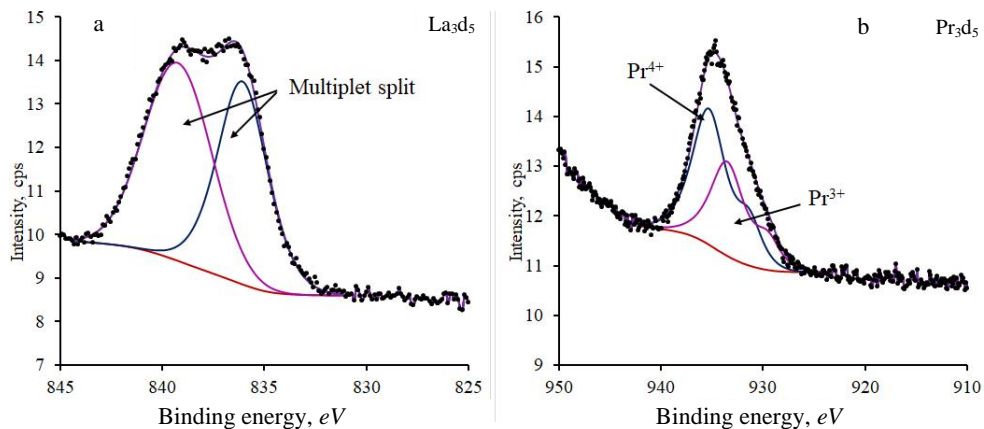


Fig. 5. XPS spectra of La 3d<sub>5/2</sub> (a), and Pr 3d<sub>5/2</sub> (b).

Fig. 5, a and b shows the X-ray photoelectron spectra of the 3d<sub>5/2</sub> levels of La and Pr borides, respectively. The obtained data are compared with NIST data. In all cases, it can be argued that the metals in the surface layer are in an oxidized state. Lanthanum has two almost equal peaks in intensity. The high-energy peak at

839.5 eV corresponds to the oxidized state of lanthanum. Since the XRD analysis showed (Fig. 1) the presence of the LaBO<sub>3</sub> phase, and EDS (Fig. 4, c) showed the presence of oxygen, this peak can be attributed to lanthanum borate, and the low-energy peak to lanthanum boride. XPS analysis of praseodymium (Pr) boride showed the presence of two peaks with energies of 935.2 eV and 933.3 eV. The first peak can be attributed to Pr<sup>4+</sup> and the second – to Pr<sup>3+</sup> in the borate compound that invisible in the XRD pattern of the PrB<sub>6</sub> sample (Fig. 3-a). The presence of oxygen is also detected in the EDS spectra (Fig. 4, d). When comparing the data of XRD analysis with XPS, it can be said that the intensities of the diffraction lines of borate structures are rather weak compared to boride lines and in XPS approximately the same intensity, from which it can be assumed that the borate structures are in the near-surface layer of the crystal, as the XPS analysis only allows probing of a ~5 nm surface layer of the samples.

**Conclusion.** This study demonstrates the feasibility of synthesizing rare-earth hexaborides via microwave-assisted solid-state reactions. Despite the thermodynamic limitations of R<sub>2</sub>O<sub>3</sub>/B systems, LaB<sub>6</sub> and PrB<sub>6</sub> were obtained as highly crystalline cubic phases with uniform morphologies and particle sizes of 1–5  $\mu\text{m}$ . For heavier lanthanides (Gd, Ho, Er), the main products were mixed boride and borate phases, indicating the increasing synthesis difficulty with increasing atomic number. XPS confirmed that the borate species are localized in the near-surface layers rather than in the bulk structure.

The developed microwave-assisted method enables the synthesis of rare-earth borides within dramatically short times (10 min), at significantly lower processing temperatures and with simple, inexpensive precursors. While pure hexaboride phases were achieved only for La and Pr, the results highlight both the potential and limitations of this approach for heavier lanthanides. These findings provide a foundation for further optimization strategies aimed at extending the scope of microwave-assisted synthesis to late lanthanide borides.

Received 28.08.2025  
Reviewed 06.10.2025  
Accepted 10.10.2025

## REFERENCES

1. Peschmann K.R., Calow J.T., Knauff K.G. Diagnosis of the Optical Properties and Structure of Lanthanum Hexaboride Thin Films. *J. Appl. Phys.* **44** (1973), 2252.  
<https://doi.org/10.1063/1.1662545>
2. Friz G.G., Wood K.S., et al. Thermoelectric Single-photon Detectors for X-ray/UV Radiation. *Proc. SPIE* **4140** (2000), 459.  
<https://doi.org/10.1117/12.409144>
3. Lafferty J.M. Boride Cathodes. *J. Appl. Phys.* **22** (1951), 299.  
<https://doi.org/10.1063/1.1699946>
4. Selvan R.K., Genish I., et al. Single Step, Low Temperature Synthesis of Submicron-Sized Rare Earth Hexaborides. *J. Phys. Chem. C* **112** (2008), 1795.  
<https://doi.org/10.1021/jp0765502>
5. Fu C., Xu J., et al. Flexible Three Dimensional CeB<sub>6</sub> Nanowire Arrays, and Excellent Field Emission Emitters. *J. Alloy. Compd.* **729** (2017), 997–1003.  
<https://doi.org/10.1016/j.jallcom.2017.09.240>

## 92 MICROWAVE-ASSISTED SYNTHESIS OF LANTHANIDE HEXABORIDES: FORMATION OF $\text{LaB}_6$ ...

---

6. Bauccio M.L. *ASM Engineered Materials Reference Book*. USA, ASM International (1994).
7. Broers A.N. Some Experimental and Estimated Characteristics of the Lanthanum Hexaboride Rod Cathode Electron Gun. *J. Phys. E, Sci. Instrum.* **2** (1969), 273.  
<https://doi.org/10.1088/0022-3735/2/3/310>
8. Sani E., Mercatelli L., et al. Lanthanum Hexaboride for Solar Energy Applications. *Sci. Reports* **7** (2017), 718.  
<https://doi.org/10.1038/s41598-017-00749-w>
9. Bliznakov G., Peshev P. The Preparation of Cerium, Praseodymium, and Neodymium Hexaborides. *J. Less-Common Met.* **7** (1964), 441–446.  
[https://doi.org/10.1016/0022-5088\(64\)90041-4](https://doi.org/10.1016/0022-5088(64)90041-4)
10. Latini A., Di Pascasio F., Gozzi D. A New Synthesis Route to Light Lanthanide Borides: Borothermic Reduction of Oxides Enhanced by Electron Beam Bombardment. *J. Alloys Compd.* **346** (2002), 311–313.  
[https://doi.org/10.1016/S0925-8388\(02\)00667-9](https://doi.org/10.1016/S0925-8388(02)00667-9)
11. Hasan M., Sugo H., Kisi E. Low Temperature Carbothermal and Boron Carbide Reduction Synthesis of  $\text{LaB}_6$ . *J. Alloys Compd.* **578** (2013), 176–182.  
<https://doi.org/10.1016/j.jallcom.2013.05.008>
12. Liu Y., Lu W.J., et al. A New Route for the Synthesis of  $\text{NdB}_6$  Powder from  $\text{Nd}_2\text{O}_3$ – $\text{B}_4\text{C}$  System. *J. Alloys Compd.* **431** (2007), 337–341.  
<https://doi.org/10.1016/j.jallcom.2006.05.084>
13. Samsonov G.V., Paderno Y.B., Fomenko V.S. Hexaborides of the Rare-earth Metals. *Powder Metall Met. Ceram.* **2** (1963), 449–454.  
<https://doi.org/10.1007/bf00774188>
14. Amalajyothi K., John L. et al. Electrosynthesis of Cerium Hexaboride by the Molten Salt Technique. *J. Cryst. Growth* **310** (2008), 3376–3379.  
<https://doi.org/10.1016/j.jcrysgro.2008.04.026>
15. Berchmans L.J., Visuvasam A. et al. Electrosynthesis of Samarium Hexaboride Using Tetra Borate Melt. *Ionics* **16** (2010), 833–838.  
<https://doi.org/10.1007/s11581-010-0469-3>
16. Uchida K., Shiota M. Electrodeposited Mixed Hexaborides of Sodium and Lanthanum. *J. Surf. Technol.* **7** (1978), 299–304.  
[https://doi.org/10.1016/0376-4583\(78\)90071-7](https://doi.org/10.1016/0376-4583(78)90071-7)
17. Xu J.Q., Zhao Y.M., Zhang Q.Y. Enhanced Electron Field Emission from Single Crystalline  $\text{LaB}_6$  Nanowires with Ambient Temperature. *J. Appl. Phys.* **104** (2008), 124306.  
<http://dx.doi.org/10.1063/1.3048547>
18. Zhang Q.Y., Xu J.Q., et al. Fabrication of Large-Scale Single Crystalline  $\text{PrB}_6$  Nanorods and Their Temperature-Dependent Electron Field Emission. *J. Adv. Funct. Mater.* **19** (2009), 742–747.  
<https://doi.org/10.1002/adfm.200801248>
19. Zhang H., Zhang Q., et al. Qin, Single-Crystalline  $\text{CeB}_6$  Nanowires. *J. Am. Chem. Soc.* **127** (2005), 8002–8003.  
<https://doi.org/10.1021/ja051340t>
20. Kher S.S., Spencer J.T. Chemical Vapor Deposition of Metal Borides: 7. The Relatively Low Temperature Formation of Crystalline Lanthanum Hexaboride Thin Films from Boron Hydride Cluster Compounds by Chemical Vapor Deposition. *J. Phys. Chem. Solids* **59** (1998), 1343–1351.  
[https://doi.org/10.1016/S0022-3697\(97\)00230-8](https://doi.org/10.1016/S0022-3697(97)00230-8)
21. Brewer J.R., Deo N., et al. Lanthanum Hexaboride Nanoobelisks. *J. Chem. Mater.* **19** (2007), 6379–6381.  
<https://doi.org/10.1021/cm702315x>
22. Selvan R.K., Genish I., et al. Single Step, Low-temperature Synthesis of Submicron-Sized Rare Earth Hexaborides. *J. Phys. Chem. C* **112** (2008), 1795–1802.  
<https://doi.org/10.1021/jp0765502>
23. Dou Z., Zhang T., et al. Preparation and Characterization of  $\text{LaB}_6$  Ultra Fine Powder by Combustion Synthesis. *Trans. Nonferrous Met. Soc. China* **21** (2011), 1790–1794.  
[https://doi.org/10.1016/S1003-6326\(11\)60932-1](https://doi.org/10.1016/S1003-6326(11)60932-1)
24. Dou Z.H., Zhang T.A., et al. He, Preparation and Characterization of Cerium Hexaboride Nanometer Powders by Combustion Synthesis. *Adv. Mater. Res.* **236–238** (2011), 1670–1674.  
<https://doi.org/10.4028/www.scientific.net/AMR.236-238.1670>

25. Bliznakov G., Peshev P. The Preparation of Cerium, Praseodymium, and Neodymium Hexaborides *J. Less Common. Met.* **7** (1964), 441–446.  
[https://doi.org/10.1016/0022-5088\(64\)90041-4](https://doi.org/10.1016/0022-5088(64)90041-4)
26. Samsonov G.V., Paderno Yu.B., Fomenko V.S. Hexaborides of the Rare-earth Metals. *Sov. Powder Metall. Metal Ceram.* **2** (1963), 449–454.  
<https://doi.org/10.1007/BF00774188>
27. Amalajyothi L., Berchmans J., et al. Novel Synthesis of Cerium Hexaboride by Hexamine Route. *Int. J. of Self-Propagating High-Temp. Synt.* **17** (2008), 218–221.  
<https://doi.org/10.3103/S106138620804002X>
28. Stuerga D.A.C., Gaillard P. Microwave Athermal Effects in Chemistry: A Myth's Autopsy: Part I: Historical Background and Fundamentals of Wave-Matter Interaction. *Journal of Microwave Power and Electromagnetic Energy* **31** (1996), 87–100.  
<https://doi.org/10.1080/08327823.1996.11688299>
29. Davtyan D., Mnatsakanyan R., et al. Microwave Synthesis of B<sub>4</sub>C Nanopowder for Subsequent Spark Plasma Sintering. *Journal of Materials Research and Technology* **8** (2019), 5823–5832.  
<https://doi.org/10.1016/j.jmrt.2019.09.052>
30. Mnatsakanyan R., Davtyan D., et al. Microwave-Assisted Preparation and Characterization of Anoscale Rhenium Diboride. *Ceramics International* **44** (2018), 22339–22344.  
<https://doi.org/10.1016/j.ceramint.2018.08.359>
31. Mnatsakanyan R., Aghoyan A., Davtyan D. Microwave-Assisted Synthesis of Boron Monophosphide Nanopowder. *Ceramics International* **49** (2023), 3066–3069.  
<https://doi.org/10.1016/j.ceramint.2022.10.330>
32. Stuerga D.A.C., Gaillard P. Microwave Athermal Effects in Chemistry: A Myth's Autopsy: Part II: Orienting Effects and Thermodynamic Consequences of Electric Field. *Journal of Microwave Power and Electromagnetic Energy* **31** (1996), 101–113.  
<https://doi.org/10.1080/08327823.1996.11688300>
33. Islamgaliev R.K., Zyrin A.V., et al. Oxidation of Powdered Hexaborides of Rare-earth Elements in Air. *Poroshk. Metall.* **12** (1987), 36–39 (in Russian).

#### Ա. Մ. ԱՂՈՅԱՆ

### ԼԱՆՁԱՆԻԴՆԵՐԻ ՀԵՔՍԱԲՈՐԻԴՆԵՐԻ ՄԻԿՐՈԱԼԻՔԱՅԻՆ ՍԻՆԹԵԶԸ. LaB<sub>6</sub> ԵՎ PrB<sub>6</sub> ԱՌԱՋԱՑՈՒՄԸ ԵՎ ԽՆԴԻՐՆԵՐԸ ԾԱՆՐ ԼԱՆՁԱՆԻԴՆԵՐԻ ԴԵՊՔՈՒՄ

Հազվագյուտ հողային տարրերի հեքսաբորիդները (RB<sub>6</sub>) խոստումնայից նյութեր են ֆոտոնային, էլեկտրոնային և էներգետիկ կիրառությունների համար՝ իրենց եզակի բյուրեղային և էլեկտրոնային կառուցվածքի շնորհիվ: Այնուամենայնիվ, դրանց սինթեզի ավանդական մեթոդները սահմանափակված են շատ բարձր ջերմաստիճանների, ռեակցիայի երկար ժամանակների և բարդ ելանյութերի օգտագործման անհրաժեշտությամբ: Այս աշխատանքում առաջարկվում է հեքսաբորիդների՝ RB<sub>6</sub> փոշիների ստացման արագ և էներգաարդյունավետ միկրոալիքային սինթեզի (ՄՄ) մեթոդը: Օգտագործելով պարզ և հասանելի ելանյութեր (լանժանիդային օքսիդներ և էլեմենտար բոր), հաջողությամբ սինթեզվել են լանժանի և պրոցեդիումի հեքսաբորիդները ընդամենը 10 րոպեում՝ չնայած R<sub>2</sub>O<sub>3</sub>/B → RB<sub>6</sub> ռեակցիաների թերմոդինամիկ սահմանափակումներին: Կառուցվածքային և մորֆոլոգիական ուսումնասիրությունները (XRD, XPS, SEM/EDS) հաստատել են բարձր բյուրեղային

խորանարդային հեքսաբորիդային ֆազերի առաջացումը՝ 1–5 մկմ մասնիկների չափսերով: Ավելի ծանր լանժանիդների (Gd, Ho, Er) դեպքում մաքուր հեքսաբորիդների փոխարեն դիտարկվել են խառը բորիդային և բորատային ֆազեր: Ստացված արդյունքները ցույց են տալիս միկրոալիքային սինթեզի մեջողի ներուժը՝ հաղթահարելու թերմոդինամիկական արգելքները և արագությունը՝ կերպով սինթեզելու առանձին լանժանիդների հեքսաբորիդներ շատ կարևոր ռեակցիոն ժամանակներում:

А. М. АГОЯН

МИКРОВОЛНОВЫЙ СИНТЕЗ ГЕКСАБОРИДОВ ЛАНТАНИДОВ:  
ОБРАЗОВАНИЕ  $\text{LaB}_6$ ,  $\text{PrB}_6$  И ПРОБЛЕМЫ ПРИ  
БОЛЕЕ ТЯЖЕЛЫХ ЛАНТАНИДАХ

Редкоземельные гексабориды ( $\text{RB}_6$ ) представляют собой перспективные материалы для фотонных, электронных и энергетических применений благодаря своей уникальной кристаллической и электронной структуре. Однако традиционные методы их синтеза ограничены необходимостью очень высоких температур, длительным временем реакции и использованием сложных прекурсоров. В данной работе предложен быстрый и энергоэффективный метод микроволнового синтеза (МС) для получения порошков  $\text{RB}_6$ . С использованием простых прекурсоров (оксиды лантанидов и элементный бор) были успешно получены гексабориды La и Pr всего за 10 мин, несмотря на термодинамические ограничения реакций  $\text{R}_2\text{O}_3/\text{B} \rightarrow \text{RB}_6$ . Структурные и морфологические исследования (XRD, XPS, SEM/EDS) подтвердили образование высококристаллических кубических фаз с однородными частицами размером 1–5 мкм. Для более тяжелых лантанидов (Gd, Ho, Er) вместо чистых гексаборидов наблюдались смешанные боридные и боратные фазы. Полученные результаты демонстрируют потенциал метода МС для преодоления термодинамических барьеров и быстрого, энергоэффективного синтеза отдельных лантанидных гексаборидов.